Could the Excess Seen at 124–126 GeV Be due to the Randall-Sundrum Radion?

Kingman Cheung[1,2] and Tzu-Chiang Yuan[3]

[1]*Department of Physics, National Tsing Hua University, Hsinchu 300, Taiwan*
[2]*Division of Quantum Phases and Devices, School of Physics, Konkuk University, Seoul 143-701, Republic of Korea*
[3]*Institute of Physics, Academia Sinica, Nangang, Taipei 11529, Taiwan*

(Received 28 December 2011; published 6 April 2012)

Current Higgs boson searches in various channels at the LHC point to an excess at around 124–126 GeV due to a possibly standard-model-like Higgs boson. If one examines more closely the channels ($\gamma\gamma$, WW^*, and ZZ^*) that have excess, this "Higgs boson" may be the Randall-Sundrum radion ϕ. Because of the trace anomaly, the radion has stronger couplings to the photon and gluon pairs. Thus, it will enhance the production rates into gg and $\gamma\gamma$, while those for WW^*, ZZ^*, and $b\bar{b}$ are reduced relative to their standard model values. We show that it can match well with the data from CMS for $m_\phi = 124$ GeV, and the required scale $\Lambda_\phi \sim \langle\phi\rangle$ is about 0.68 TeV.

DOI: 10.1103/PhysRevLett.108.141602 PACS numbers: 11.25.Mj, 11.10.Kk, 14.80.Ec

Introduction.—With tremendous speculations before December 13, 2011, the first glimpse of the Higgs boson was revealed on that day. Both ATLAS [1] and CMS [2] saw some excess of events of the Higgs decays in the $H \to \gamma\gamma$, $H \to WW^* \to \ell\nu\ell\nu$, and $H \to ZZ^* \to 4\ell$ channels. If one examines more closely these channels, one may notice that the excessive channels exhibit some correlations, even though it is still too early to say anything concrete. According to the CMS data [2] for the Higgs mass $m_H = 124$ GeV, the excess relative to the corresponding standard model (SM) values are

$$\begin{aligned}
\sigma(H)B(H \to b\bar{b})/\sigma B_{\rm SM} &\sim 1.1^{+1.5}_{-1.6}, \\
\sigma(H)B(H \to \tau\tau)/\sigma B_{\rm SM} &\sim 0.8^{+1.2}_{-1.3}, \\
\sigma(H)B(H \to \gamma\gamma)/\sigma B_{\rm SM} &\sim 2.1^{+0.6}_{-0.7}, \\
\sigma(H)B(H \to WW^*)/\sigma B_{\rm SM} &\sim 0.7^{+0.4}_{-0.6}, \\
\sigma(H)B(H \to ZZ^* \to 4\ell)/\sigma B_{\rm SM} &\sim 0.5^{+1.1}_{-0.7},
\end{aligned} \tag{1}$$

where $\sigma B_{\rm SM}$ denotes the cross section $\sigma(H)$ times the corresponding branching ratio for the SM. (ATLAS [1] also has the ratio of $\gamma\gamma$ production rate larger than the SM one.) At face value, except for the $\gamma\gamma$ channel, almost all are slightly suppressed relative to the SM cross sections. Note that these results consist of large errors. If we take these numbers seriously, the branching ratios of the 124–126 GeV "Higgs boson" observed have to be modified. One possible way is to add an unobserved channel, e.g., dijet or invisible particles, such that the Higgs decays into $b\bar{b}$, $\tau\tau$, WW^*, and ZZ^* are reduced, while at the same time the $\gamma\gamma$ channel has to be enhanced by a relatively large amount. In this work, we point out that the Randall-Sundrum (RS) radion, with enhanced couplings to gg and $\gamma\gamma$ due to a trace anomaly, can explain the ratios in Eq. (1). Also, the radion can give rise to enhanced dijet production at 124–126 GeV. The associated production with a W or a Z boson may be observable. The radion provides an alternative and the most economical solution to explain the observed rates. This is the main result of this work.

A large number of works appeared to interpret the 124–126 GeV Higgs boson in the minimal supersymmetric standard model (MSSM) framework [3], in the next-to-minimal supersymmetric standard model (NMSSM) framework [4], in the two-Higgs-doublet model [5], in other supersymmetry framework [6], and others [7].

The radion.—The RS model [8] that uses a warped space-time in a slice of extra dimension explains the gauge hierarchy problem well. The RS model has a four-dimensional massless scalar, the modulus or radion [9–11], about the background geometry:

$$ds^2 = e^{-2k|\varphi|T(x)} g_{\mu\nu}(x) dx^\mu dx^\nu - T^2(x) d\varphi^2,$$

where $g_{\mu\nu}(x)$ is the four-dimensional graviton and $T(x)$ is the modulus field. The most important ingredients of the above brane configuration for phenomenological studies are the required size of the modulus field such that it generates the desired weak scale from the high scale M and the stabilization of the modulus field at this value. A stabilization mechanism was proposed by Goldberger and Wise [9] that a bulk scalar field propagating in the background solution of the metric can generate a potential that can stabilize the modulus field. The minimum of the potential can be arranged to give the desired value of kr_c without fine-tuning of parameters. It has been shown [10] that if a large value of $kr_c \sim 12$, needed to solve the hierarchy problem, arises from a small bulk scalar mass, then the modulus potential near its minimum is nearly flat for values of the modulus vacuum expectation value that solves the hierarchy problem. As a consequence, besides getting a mass, the modulus field is likely to be lighter than any Kaluza-Klein modes of any bulk field. The lightest mode is the radion, which has a mass of the order of 100 GeV to a TeV, and the strength of its coupling to the

SM fields is of the order of $O(1/\mathrm{TeV})$. There is no theoretical preferred mass region for the radion, and it was shown in Ref. [12] that the unmixed radion is consistent with electroweak precision data. Therefore, the detection of this radion may be the first signature of the RS model.

The interactions of the radion ϕ with the SM particles on the brane are model-independent and are governed by four-dimensional general covariance given by the following Lagrangian:

$$\mathcal{L}_{\mathrm{int}} = \frac{\phi}{\Lambda_\phi} T^\mu_\mu(\mathrm{SM}), \tag{2}$$

where $\Lambda_\phi = \langle\phi\rangle$ is of the order of TeV and T^μ_μ is the trace of the SM energy-momentum tensor, which is given by

$$T^\mu_\mu(\mathrm{SM}) = \sum_f m_f \bar{f} f - 2m_W^2 W^+_\mu W^{-\mu} - m_Z^2 Z_\mu Z^\mu + (2m_H^2 H^2 - \partial_\mu H \partial^\mu H) + \cdots, \tag{3}$$

where $\cdots$ denotes higher order terms. The couplings of the radion with fermions f, gauge bosons W and Z, and Higgs boson H are completely fixed by Eq. (2).

For the coupling of the radion to a pair of gluons (photons), there are contributions from 1-loop diagrams with the top quark (top quark and W) in the loop as well as from the trace anomaly. The contribution from the trace anomaly for gauge fields is given by

$$T^\mu_\mu(\mathrm{SM})^{\mathrm{anom}} = \sum_a \frac{\beta_a(g_a)}{2g_a} F^a_{\mu\nu} F^{a\mu\nu}. \tag{4}$$

For QCD, $\beta_{\mathrm{QCD}}/2g_s = -(\alpha_s/8\pi) b_{\mathrm{QCD}}$, where $b_{\mathrm{QCD}} = 11 - 2n_f/3$ with $n_f = 6$. Thus, the effective coupling of $\phi g(p_1) g(p_2)$, including the 1-loop diagrams of the top quark and the trace anomaly contributions, is given by

$$\frac{i\delta_{ab}\alpha_s}{2\pi\Lambda_\phi}\{b_{\mathrm{QCD}} + y_t[1 + (1 - y_t) f(y_t)]\} \times (p_1 \cdot p_2 g_{\mu\nu} - p_{2_\mu} p_{1_\nu}), \tag{5}$$

where $y_t = 4m_t^2/2p_1 \cdot p_2$ with the gluon incoming momenta p_1 and p_2. Similarly, the effective coupling of $\phi\gamma(p_1)\gamma(p_2)$, including the 1-loop diagrams of the top quark and W boson and the trace anomaly contributions, is given by

$$\frac{i\alpha_{\mathrm{em}}}{2\pi\Lambda_\phi}\Big\{b_2 + b_Y - [2 + 3y_W + 3y_W(2 - y_W) f(y_W)] + \frac{8}{3} y_t[1 + (1 - y_t) f(y_t)]\Big\}(p_1 \cdot p_2 g_{\mu\nu} - p_{2_\mu} p_{1_\nu}), \tag{6}$$

where $b_2 = 19/6$, $b_Y = -41/6$, and $y_i = 4m_i^2/2p_1 \cdot p_2$ with $i = W, t$. In the above Eqs. (5) and (6), the function $f(z)$ is given by

$$f(z) = \begin{cases} \left[\sin^{-1}\left(\frac{1}{\sqrt{z}}\right)\right]^2, & z \geq 1, \\ -\frac{1}{4}\left[\log\left(\frac{1+\sqrt{1-z}}{1-\sqrt{1-z}}\right) - i\pi\right]^2, & z < 1. \end{cases}$$

There have been many phenomenological studies of the radion or dilaton at colliders [13] in the literature. More recent works related to the LHC can be found in Ref. [14].

Decays and production of the radion.—With the above interactions, we can calculate the partial widths of the radion into gg, $\gamma\gamma$, $f\bar{f}$, W^+W^-, ZZ, and HH. The partial widths are given by

$$\Gamma(\phi \to gg) = \frac{\alpha_s^2 m_\phi^3}{32\pi^3\Lambda_\phi^2} |b_{\mathrm{QCD}} + x_t[1 + (1 - x_t) f(x_t)]|^2, \tag{7}$$

$$\Gamma(\phi \to \gamma\gamma) = \frac{\alpha_{\mathrm{em}}^2 m_\phi^3}{256\pi^3\Lambda_\phi^2} |b_2 + b_Y - [2 + 3x_W + 3x_W(2 - x_W) f(x_W)] + \frac{8}{3} x_t[1 + (1 - x_t) f(x_t)]|^2, \tag{8}$$

$$\Gamma(\phi \to f\bar{f}) = \frac{N_c m_f^2 m_\phi}{8\pi\Lambda_\phi^2}(1 - x_f)^{3/2}, \tag{9}$$

$$\Gamma(\phi \to W^+W^-) = \frac{m_\phi^3}{16\pi\Lambda_\phi^2}\sqrt{1 - x_W}\left(1 - x_W + \frac{3}{4}x_W^2\right), \tag{10}$$

$$\Gamma(\phi \to ZZ) = \frac{m_\phi^3}{32\pi\Lambda_\phi^2}\sqrt{1 - x_Z}\left(1 - x_Z + \frac{3}{4}x_Z^2\right), \tag{11}$$

$$\Gamma(\phi \to HH) = \frac{m_\phi^3}{32\pi\Lambda_\phi^2}\sqrt{1 - x_H}\left(1 + \frac{x_H}{2}\right)^2, \tag{12}$$

TABLE I. The branching ratios of the RS radion for $m_\phi = 123$–126 GeV.

m_ϕ	Branching ratios					
(GeV)	gg	$b\bar{b}$	$\tau\tau$	WW^*	ZZ^*	$\gamma\gamma$
123	0.899	0.0608	9.49×10^{-3}	0.0246	2.93×10^{-3}	0.912×10^{-3}
124	0.897	0.0598	9.34×10^{-3}	0.0267	3.25×10^{-3}	0.918×10^{-3}
125	0.896	0.0588	9.2×10^{-3}	0.0291	3.6×10^{-3}	0.925×10^{-3}
126	0.894	0.0578	9.05×10^{-3}	0.0317	3.98×10^{-3}	0.931×10^{-3}

TABLE II. A few production cross sections and branching ratios of the SM Higgs boson for $m_H = 123$–126 GeV. We borrow the values from Ref. [15].

m_H	Cross sections (pb)			Branching ratios				
(GeV)	$gg \to H$	WH	ZH	$b\bar{b}$	$\tau\tau$	WW^*	ZZ^*	$\gamma\gamma$
123	15.8	0.61	0.33	0.607	0.067	0.185	0.022	2.28×10^{-3}
124	15.6	0.59	0.32	0.592	0.065	0.200	0.0242	2.29×10^{-3}
125	15.3	0.57	0.32	0.577	0.064	0.216	0.0266	2.29×10^{-3}
126	15.1	0.56	0.31	0.561	0.062	0.233	0.0291	2.29×10^{-3}

where $x_i = 4m_i^2/m_\phi^2$ ($i = f, W, Z, H$) and $N_c = 3$ (1) for quarks (leptons). Note that the branching ratios are independent of Λ_ϕ.

In calculating the partial widths into fermions, we have used the 3-loop running masses with scale $Q^2 = m_\phi^2$. We have also allowed the off-shell decays of the W and Z bosons and that of the top quark. The features of radion decay branching ratios are similar to the decay of the Higgs boson, except the following. At $m_\phi \lesssim 140$ GeV, the decay width is dominated by $\phi \to gg$, while the decay width of the SM Higgs boson is dominated by the $b\bar{b}$ mode. At larger m_ϕ, ϕ also decays into a pair of Higgs bosons ($\phi \to HH$) if kinematically allowed, while the SM Higgs boson cannot. Similar to the SM Higgs boson, as m_ϕ goes beyond the WW and ZZ thresholds, the WW and ZZ modes dominate with the WW partial width about a factor of 2 of the ZZ partial width. We list the relevant branching ratios of the radion in Table I for $m_\phi = 123$–126 GeV. Just for comparison with the SM Higgs boson, we also list the branching ratios and production cross sections of the SM Higgs boson in Table II (from Ref. [15]).

The production channels of the radion at hadronic colliders include

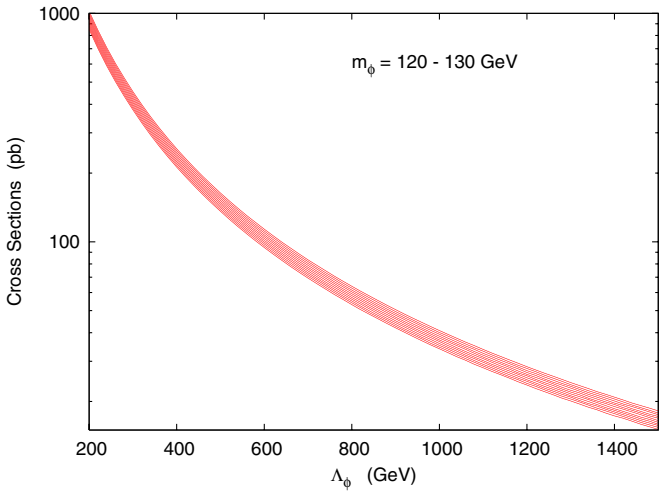

FIG. 1 (color online). Production cross sections for $pp \to \phi$ via gluon fusion versus Λ_ϕ for $m_\phi = 120$–130 GeV. The top of the "thick" curve is for 120 GeV, while the bottom is for 130 GeV.

$$gg \to \phi, \qquad q\bar{q}' \to W\phi, \qquad q\bar{q} \to Z\phi,$$
$$qq' \to qq'\phi \ (WW, ZZ \text{ fusion}), \qquad q\bar{q}, gg \to t\bar{t}\phi.$$

Similar to the SM Higgs boson, the most important production channel for the radion is gg fusion. In addition, $gg \to \phi$ gets further enhancement from the trace anomaly. We shall consider only the gluon fusion in the following. We show the production cross sections for $m_\phi = 120$–130 GeV versus Λ_ϕ in Fig. 1.

Comparison to the LHC data.—Using the appropriate entries from Tables I and II for $m_{\phi/H} = 124$ GeV, we can compute the following ratio:

$$\frac{\sigma(\phi)B(\phi \to \gamma\gamma)}{\sigma(H)B(H \to \gamma\gamma)} = \frac{\sigma(\phi) \times 0.918 \times 10^{-3}}{15.6\,\text{pb} \times 2.29 \times 10^{-3}} = 2.1, \quad (13)$$

where 2.1 is the central value of the CMS data [2] for this ratio. Therefore, the value of $\sigma(\phi)$ obtained in the above equation is 82 pb, which corresponds to $\Lambda_\phi = 0.68$ TeV from Fig. 1. If we use the diphoton data with error bars $(2.1^{+0.6}_{-0.7})$, the corresponding $\Lambda = 0.68^{+0.15}_{-0.08}$ TeV. Once the ratio for $\gamma\gamma$ is fixed, the other ratios can be easily obtained by using Tables I and II:

$$\frac{\sigma(\phi)B(\phi \to b\bar{b})}{\sigma(H)B(H \to b\bar{b})} = \frac{82\ \text{pb} \times 0.0598}{15.6\ \text{pb} \times 0.592} = 0.53, \quad (14)$$

$$\frac{\sigma(\phi)B(\phi \to \tau\tau)}{\sigma(H)B(H \to \tau\tau)} = \frac{82\ \text{pb} \times 9.34 \times 10^{-3}}{15.6\ \text{pb} \times 0.065} = 0.75, \quad (15)$$

$$\frac{\sigma(\phi)B(\phi \to WW^*)}{\sigma(H)B(H \to WW^*)} = \frac{82\ \text{pb} \times 0.0267}{15.6\ \text{pb} \times 0.200} = 0.70, \quad (16)$$

TABLE III. The ratio $\frac{\sigma(\phi)B(\phi \to X)}{\sigma(H)B(H \to X)}$ for $m_{\phi \text{ or } H} = 123$–$126$ GeV.

$m_{\phi \text{ or } H}$	$\frac{\sigma(\phi)B(\phi \to X)}{\sigma(H)B(H \to X)}$				
(GeV)	$\gamma\gamma$	$b\bar{b}$	$\tau\tau$	WW^*	ZZ^*
123	2.1	0.53	0.74	0.70	0.70
124	2.1	0.53	0.75	0.70	0.70
125	2.1	0.53	0.75	0.70	0.70
126	2.1	0.53	0.75	0.70	0.71

TABLE IV. Production cross sections in femtobarns for $\sigma(W\phi \to Wgg)$ and $\sigma(Z\phi \to Zgg)$ at the Tevatron and at the LHC-7. The Λ_ϕ is set at 0.68 TeV.

m_ϕ	$\sigma(W\phi)B(\phi \to gg)$		$\sigma(Z\phi)B(\phi \to gg)$	
(GeV)	Tevatron	LHC-7	Tevatron	LHC-7
123	19.1	73.4	11.5	39.1
124	18.5	71.2	11.1	38.0
125	17.9	69.2	10.8	36.9
126	17.4	67.1	10.5	35.8

$$\frac{\sigma(\phi)B(\phi \to ZZ^*)}{\sigma(H)B(H \to ZZ^*)} = \frac{82\,\text{pb} \times 3.25 \times 10^{-3}}{15.6\,\text{pb} \times 0.0242} = 0.70. \quad (17)$$

Therefore, we obtain a set of ratios which match well with the central values of the CMS data, provided that we first match the $\gamma\gamma$ mode to the experimental data. We repeat the exercise for other $m_\phi = 123$–126 GeV with the results shown in Table III. The ratios vary very little in this radion mass range.

Implications.—The radion has a large branching ratio into gg, which will give rise to a dijet signal at the Tevatron and the LHC. The cross section $\sigma(gg \to \phi)B(\phi \to gg) \approx 73$ pb at the LHC and only 3.4 pb at the Tevatron. The huge QCD background will overwhelm the dijet signal. The only possibility is to consider the associated production with a W or a Z boson. In Table IV, we calculate the production cross section of $W\phi$ and $Z\phi$ at the Tevatron and at the LHC, multiplied by the gluonic branching ratio. With this level of cross sections it is still difficult to beat the Wjj and Zjj background. If the systematics can be reduced to a few percent level, it may have some chance to see this dijet signal.

In conclusion, the CMS and ATLAS Collaborations have seen excess in a number of channels; in particular, the $\gamma\gamma$ channel has a cross section about twice the SM value, while the other channels are slightly suppressed (by about 0.5–0.7) relative to their SM values. We have proposed the RS radion as a possible candidate for the particle observed. While it is not easy to accommodate a 125 GeV Higgs boson with an enhanced diphoton rate in the MSSM [3], NMSSM [4], and a number of other popular models [16–18], the RS radion provides the most economical way to interpret the data. In order to give a 124–126 GeV Higgs boson within MSSM, the stop sector must consist of a large mixing that gives rise to one very heavy stop $\tilde{t}_2$ and one relatively light stop $\tilde{t}_1$. Within the MSSM and NMSSM, it is rather difficult to enhance the $\gamma\gamma$ production rate [3,4]; only in some less restrictive NMSSM can the rate be enhanced by a factor up to 2 [4]. The littlest Higgs model [16] always gives a slight reduction in the diphoton rate. The inert Higgs doublet model [17] gives a diphoton rate in the range of 0.8–1.3 relative to the SM rate, but it can hardly go over 1.5. In a type-II seesaw model [18], the diphoton production rate can be enhanced significantly because of the contribution from the double-charged Higgs boson but at relatively large values of self-couplings. The radion, due to the trace anomaly, has enhanced couplings to a pair of photons and gluons. Thus, the production rate of $\sigma(\phi)B(\phi \to \gamma\gamma)$ can be enhanced relative to the SM cross section. The data requires $\Lambda_\phi \approx 0.68$ TeV. At the same time, the other channels $b\bar{b}$, $\tau\tau$, WW, and ZZ are all suppressed by a factor of 0.5–0.7 (shown in Table III) relative to the SM. Therefore, the RS radion provides a reasonably good interpretation to the data. Such a radion will give rise to a large dijet resonance signal, though it is still very difficult to identify it in the presence of huge QCD background, unless the systematic uncertainty can be reduced to a few percent level.

This work was supported in part by the National Science Council of Taiwan under Grants No. 99-2112-M-007-005-MY3 and No. 98-2112-M-001-014-MY3 as well as the WCU program through the KOSEF funded by the MEST (R31-2008-000-10057-0).

[1] ATLAS Collaboration, arXiv:1202.1408 [Phys. Lett. B (to be published)]; Report No. ATLAS-CONF-2011-163, 2011.
[2] CMS Collaboration, arXiv:1202.1488; CMS PAS HIG-11-032, 2011.
[3] L. J. Hall, D. Pinner, and J. T. Ruderman, arXiv:1112.2703; H. Baer, V. Barger, and A. Mustafayev, arXiv:1112.3017; J. L. Feng, K. T. Matchev, and D. Sanford, arXiv:1112.3021; S. Heinemeyer, O. Stal, and G. Weiglein, arXiv:1112.3026; A. Arbey, M. Battaglia, A. Djouadi, F. Mahmoudi, and J. Quevillon, Phys. Lett. B **708**, 162 (2012); A. Arbey, M. Battaglia, and F. Mahmoudi, arXiv:1112.3032 [Eur. Phys. J. C (to be published)]; P. Draper, P. Meade, M. Reece, and D. Shih, arXiv:1112.3068; T. Moroi and K. Nakayama, arXiv:1112.3123; M. Carena, S. Gori, N. R. Shah, and C. E. M. Wagner, arXiv:1112.3336; O. Buchmueller *et al.*, arXiv:1112.3564; S. Akula, B. Altunkaynak, D. Feldman, P. Nath, and G. Peim, Phys. Rev. D **85**, 075001 (2012); M. Kadastik, K. Kannike, A. Racioppi, and M. Raidal, arXiv:1112.3647.
[4] U. Ellwanger, arXiv:1112.3548 [J. High Energy Phys. (to be published)]; J. F. Gunion, Y. Jiang, and S. Kraml, arXiv:1201.0982.
[5] P. M. Ferreira, R. Santos, M. Sher, and J. P. Silva, arXiv:1112.3277.
[6] T. Li, J. A. Maxin, D. V. Nanopoulos, and J. W. Walker, arXiv:1112.3024; T. Moroi, R. Sato, and T. T. Yanagida, arXiv:1112.3142 [Phys. Lett. B (to be published)].
[7] A. Djouadi, O. Lebedev, Y. Mambrini, and J. Quevillon, arXiv:1112.3299; Z.-z. Xing, H. Zhang, and S. Zhou, arXiv:1112.3112; C. Cheung and Y. Nomura, arXiv:1112.3043; J. Elias-Miro, J. R. Espinosa, G. F. Giudice, G. Isidori, A. Riotto, and A. Strumia, arXiv:1112.3022; G. Guo, B. Ren, and X.-G. He, arXiv:1112.3188; C. Englert, T. Plehn, D. Zerwas, and P. M. Zerwas, Phys. Lett. B **703**, 298 (2011); I. Gogoladze,

Q. Shafi, and C. S. Un, arXiv:1112.2206; S. Baek, P. Ko, and W.-I. Park, arXiv:1112.1847 [J. High Energy Phys. (to be published)]; I. Masina and A. Notari, arXiv:1112.2659.

[8] L. Randall and R. Sundrum, Phys. Rev. Lett. **83**, 3370 (1999); **83**, 4690 (1999).

[9] W. Goldberger and M. Wise, Phys. Rev. Lett. **83**, 4922 (1999).

[10] W. Goldberger and M. Wise, Phys. Lett. B **475**, 275 (2000).

[11] C. Csáki, M. Graesser, L. Randall, and J. Terning, Phys. Rev. D **62**, 045015 (2000); C. Csáki, M. Graesser, and G. Kribs, Phys. Rev. D **63**, 065002 (2001).

[12] J. F. Gunion, M. Toharia, and J. D. Wells, Phys. Lett. B **585**, 295 (2004).

[13] See, for example, K.-m. Cheung, Phys. Rev. D **63**, 056007 (2001); S. Bae, P. Ko, H. S. Lee, and J. Lee, Phys. Lett. B **487**, 299 (2000); S. C. Park, H. S. Song, and J.-H. Song, Phys. Rev. D **63**, 077701 (2001); J. F. Gunion, M. Toharia, and J. D. Wells, Phys. Lett. B **585**, 295 (2004); J. L. Hewett and T. G. Rizzo, J. High Energy Phys. 08 (**2003**) 028; T. Han, G. D. Kribs, and B. McElrath, Phys. Rev. D **64**, 076003 (2001); C. Csáki, J. Hubisz, and S. J. Lee, Phys. Rev. D **76**, 125015 (2007); W. D. Goldberger, B. Grinstein, and W. Skiba, Phys. Rev. Lett. **100**, 111802 (2008).

[14] Y. Eshel, S. J. Lee, G. Perez, and Y. Soreq, J. High Energy Phys. 10 (2011) 015; V. Barger and M. Ishida, arXiv:1110.6452; V. Barger, M. Ishida, and W.-Y. Keung, Phys. Rev. D **85**, 015024 (2012); arXiv:1111.4473.

[15] LHC Higgs Cross Section Working Group, *Handbook of LHC Higgs Cross Sections: 1. Inclusive Observables*, edited by S. Dittmaier, C. Mariotti, G. Passarino, and R. Tanaka (CERN, Geneva, 2011).

[16] T. Han, H. E. Logan, B. McElrath and L.-T. Wang, Phys. Lett. B **563**, 191 (2003); **603**, 257(E) (2004).

[17] A. Arhrib, R. Benbrik, and N. Gaur, arXiv:1201.2644.

[18] A. Arhrib, R. Benbrik, M. Chabab, G. Moultaka, and L. Rahili, arXiv:1112.5453.